Uncertainties in climate assessment for the case of aviation NO

Christopher D. Holmes[1], Qi Tang, and Michael J. Prather

Department of Earth System Science, University of California, Irvine, CA 92697-3100

Nitrogen oxides emitted from aircraft engines alter the chemistry of the atmosphere, perturbing the greenhouse gases methane (CH_4) and ozone (O_3). We quantify uncertainties in radiative forcing (RF) due to short-lived increases in O_3, long-lived decreases in CH_4 and O_3, and their net effect, using the ensemble of published models and a factor decomposition of each forcing. The decomposition captures major features of the ensemble, and also shows which processes drive the total uncertainty in several climate metrics. Aviation-specific factors drive most of the uncertainty for the short-lived O_3 and long-lived CH_4 RFs, but a nonaviation factor dominates for long-lived O_3. The model ensemble shows strong anticorrelation between the short-lived and long-lived RF perturbations ($R^2 = 0.87$). Uncertainty in the net RF is highly sensitive to this correlation. We reproduce the correlation and ensemble spread in one model, showing that processes controlling the background tropospheric abundance of nitrogen oxides are likely responsible for the modeling uncertainty in climate impacts from aviation.

aviation emissions | error correlation | model sensitivity

Quantifying uncertainties in climate processes is a major priority for climate research, as exemplified by the widespread use of probability distributions and uncertainties in the Intergovernmental Panel on Climate Change (IPCC) Fourth Assessment Report (1). To understand and attribute changes in the greenhouse gases and aerosols that force climate change, we rely on chemistry-transport models (CTMs), which require further characterization of their errors (e.g., 2–5). Aviation emissions are estimated to contribute 5% of anthropogenic climate forcing, with a nearly threefold uncertainty (6). This forcing occurs mainly through aviation-induced cloudiness and emissions of CO_2 and nitrogen oxides. Climate impacts of other aviation emissions—CO, SO_2, soot, hydrocarbons, and water vapor—are highly uncertain, but estimated to be much smaller (6). In this paper we quantify one type of climate forcing and its uncertainty, the impact of aviation emissions on the greenhouse gases ozone (O_3) and methane (CH_4).

Aircraft engines emit NO and NO_2 (NOx), which are indirect greenhouse gases through their chemical reactions impacting O_3 production and the CH_4 lifetime. As an O_3 precursor, NOx emissions increase the tropospheric column of O_3 and its radiative forcing. Aviation NOx emissions have a stronger impact on O_3 than surface emissions on a per molecule basis because they occur at high altitudes (7). Previous model-based estimates of the amount of O_3 generated by aviation NOx emissions vary by up to 100% and these differences have been attributed to a range of causes: e.g., the ratios of $NO:NO_2$ and $OH:HO_2$, background NOx levels (8), location and time of emissions (9–11), the amount of sunlight (12), and atmospheric mixing (13, 14).

Early work on climate forcing by aviation assumed that the impacts would be short-lived and limited to the northern latitudes containing the major flight corridors because of the short lifetime (months) of O_3. Subsequent studies, however, found that the short-lived, aviation-induced O_3 and CO perturbations propagate to the tropics where they boost OH levels and trigger a long-lived negative perturbation to global CH_4 abundance (15). An equally long-lived, global, and negative O_3 perturbation accompanies the CH_4 perturbation, and is based on numerous studies showing that

the increase in mean tropospheric O_3 since preindustrial times is partially due to the increase in CH_4 (16, 17). The negative aviation radiative forcing (RF) due to long-lived CH_4 and O_3 perturbations nearly cancels the short-lived positive RF due to O_3 (12), which creates large uncertainty in the net forcing. Although most studies find that aviation NOx emissions cause net positive RF, some find negative forcing (8, 11, 18). This work aims to quantify the RF uncertainty using two complementary approaches. Part of the analysis is similar to that in earlier studies and IPCC assessments: We look at the ensemble of published model results and perform sensitivity analyses on poorly understood processes with a single CTM. We also develop another analysis here: We decompose the RF into components and factors, assess the possible errors in each, and then propagate the final uncertainty in RF. Taken together, these approaches point to atmospheric measurements that would reduce uncertainties in key processes involved in climate forcing.

RF Uncertainty from Model Ensembles

In this section we analyze aviation NOx RF from the ensemble of all published studies since the IPCC aviation assessment (15), which synthesized earlier work. Fig. 1 shows each RF estimate from the last 12 y, broken down into its short-lived and long-lived O_3 and CH_4 components. These estimates come from diverse models, including CTMs (7, 10–12, 18–21) and coupled chemistry-climate general circulation models (GCMs) (7, 15, 19–21). They are based on a wide range of scenarios for aviation and other emissions. Studies find little evidence for nonlinearity of the atmospheric response to aviation emissions over the range 0.4 to 1.3 Tg(N) a^{-1} used in the ensemble here (7, 18), so we normalize all results to 1 Tg(N) a^{-1} from aviation.

The RF values in Fig. 1 and throughout this work are the steady-state responses to aviation NOx emissions. Most studies calculate these by the difference between two steady-state simulations with differing aviation NOx emissions (7, 18–21). Three studies report 100-year integrated RF responses to pulse emissions of aviation NOx (10–12), which are comparable to the steady-state response because the integration time is much longer than the CH_4 perturbation lifetime (10–15 y). The latter studies use pulse durations between 1 mo and 1 y, which could conceivably increase the spread of RF estimates, but we find their results to be within the envelope of RF from steady-state simulations. Our ensemble statistics would not change by excluding them. We exclude one recent aviation study (22) because its results derive from the same model simulations as another included study (21) and another because of its different experimental design (23). Stated RFs are based on composition changes in the troposphere and do not include stratospheric response, although some studies also include the lower stratosphere, where aviation NOx also increases O_3
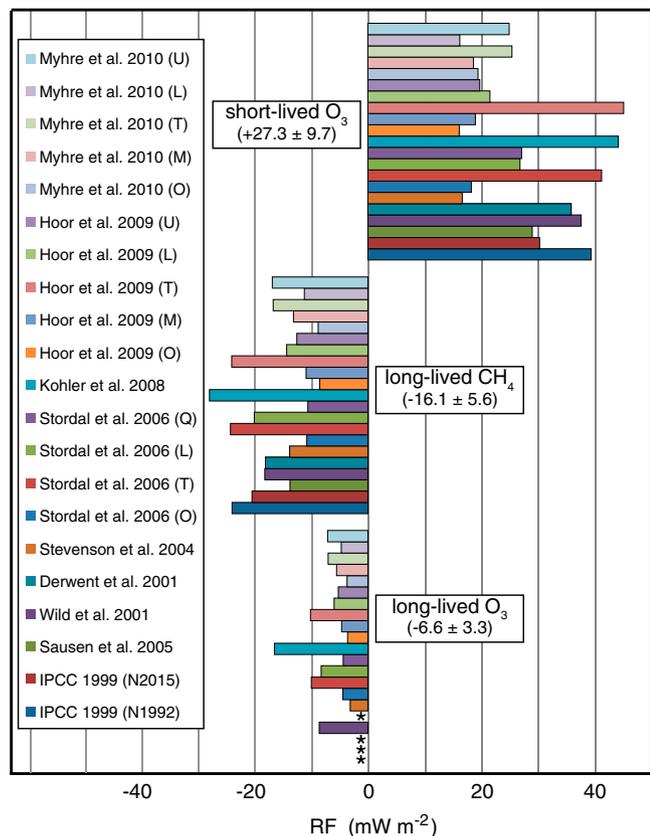
ENVIRONMENTAL SCIENCES

Fig. 1. Steady-state RF (mW m^{-2}) from short-lived O_3, long-lived CH_4, and long-lived O_3 caused by aviation NOx emissions. Values are scaled to 1 Tg(N) a^{-1}. For papers reporting multiple models or scenarios, the key is O, Oslo-CTM2; L, LMDz-INCA; M, TM4; Q, ULAQ; T, p-TOMCAT; U, UCI; N2015, NASA-2015; N1992, NASA-1992. Derwent et al. (10) is corrected by Stevenson et al. (11). An asterisk (*) indicates studies that did not report long-lived O_3 RF. The means and standard deviations are given for each of the three components.

(e.g., 15) and the greenhouse effect is similar to the upper troposphere. The CH_4 RF here also excludes changes to stratospheric water vapor, which are estimated to increase RF cooling by about 15% (24). Transient CH_4 perturbations for any particular year are always less than predicted at steady state due to the decadal lifetime of CH_4 and the steadily increasing aviation emissions (25). We use steady-state CH_4 RF here to avoid making assumptions about historical emissions and perturbations, and also because it is directly proportional to the global warming potential (GWP).

None of the three RF estimates in Fig. 1 exhibit any trends over time of publication. Likewise, their spread has not changed over a decade of model development. We find no clear differences between GCMs and CTMs in any individual RF component or in the net RF, although one of the CTMs (model T in Fig. 1) has the largest component RFs in several studies, perhaps due to its lower CO abundance and larger ozone production efficiency (7, 18, 20). At the opposite end, Unger et al. (23) find much smaller RF from short-lived O_3 that is not statistically significant and is confounded by simultaneous changes in aviation aerosols and clouds. Treating all of the data in Fig. 1 as independent samples of a normal distribution, we estimate the steady-state RF effects from 1 Tg(N) a^{-1} from aviation to be $+27.3 \pm 9.7$ mW m^{-2} due to short-lived O_3, -16.1 ± 5.6 mW m^{-2} due to long-lived CH_4, and -6.6 ± 3.3 mW m^{-2} due to long-lived O_3.

RF Uncertainty from Factor Decomposition

Past efforts to quantify the uncertainty in the climate impacts of aviation NOx have relied primarily on ensembles of model simu-

lations, as in the prior section. In this section we present an alternative method for determining the uncertainty of aviation impacts based on decomposing the RF into its key factors. We use literature review and expert judgment to assess the uncertainty in each factor and propagate these to the uncertainty in RF. Many of the factors can be derived from the general climate forcing literature and do not require model simulations that are specific to aviation. A major advantage of this approach is that we can identify the dominant sources of uncertainty.

The steady-state, global mean RF from aviation NOx emissions (F) can be broken into components due to the short-lived O_3 response ($F_{\text{short } O_3}$), and the long-lived CH_4 and O_3 responses ($F_{\text{long } CH_4}$ and $F_{\text{long } O_3}$, respectively):

$$F = F_{\text{short } O_3} + F_{\text{long } CH_4} + F_{\text{long } O_3}. \qquad [1]$$

These components can in turn be factorized into key terms summarizing the chemical interactions between NOx, O_3, and CH_4, including their feedbacks:

$$F_{\text{short } O_3} = (d[O_3]_{\text{short}}/dE)(dF/d[O_3]), \qquad [2]$$

$$F_{\text{long } CH_4} = (dL_{CH_4}/dE)f_{CH_4}[CH_4](dF/d[CH_4]), \text{ and} \qquad [3]$$

$$F_{\text{long } O_3} = (dL_{CH_4}/dE)f_{CH_4}[CH_4](d[O_3]/d[CH_4])(dF/d[O_3]), \qquad [4]$$

where $d[O_3]_{\text{short}}/dE$ is the short-lived O_3 response to aviation NOx emissions (E) and dL_{CH_4}/dE is the accompanying relative change in CH_4 lifetime, $dF/d[O_3]$ and $dF/d[CH_4]$ are the RF efficiencies of tropospheric O_3 and CH_4, $[CH_4] = 1.78$ ppm is the global mean CH_4 abundance, f_{CH_4} is the feedback factor, which prolongs the lifetime of CH_4 perturbations (16), and $d[O_3]/d[CH_4]$ is the O_3 component of the long-lived CH_4 perturbation (26). Note that the product of the first three terms on the right-hand sides of Eqs. **3** and **4** equals the steady-state response of CH_4 abundance to aviation emissions (14).

Table 1 reviews the best estimates and one-sigma uncertainties (68% confidence interval) of each factor in Eqs. **2–4**, including the values adopted in this work. Atmospheric measurements provide no direct constraints on these factors. Although the range of models does not encompass all potential uncertainties and errors, it does in this case provide a large ensemble.

Only two of the factors—$d[O_3]_{\text{short}}/dE$ and dL_{CH_4}/dE—require model simulations specific to aviation to derive their values and uncertainties, although $dF/d[O_3]$ is also somewhat dependent on the aviation perturbation (see below). The values adopted here for $d[O_3]_{\text{short}}/dE$ and dL_{CH_4}/dE encompass recent estimates based on model ensembles (19, 20), but exclude values from IPCC (15) that were based on early CTMs, which had coarse resolution at aircraft altitudes, and were not supported by subsequent studies. The poorly understood sources of model differences in these terms are discussed below, but likely involve the range of $NO:NO_2$ and $OH:HO_2$ ratios and background NOx abundances across the models.

The remaining factors can be estimated from general literature on atmospheric composition and climate, without requiring model studies or calculations specific to aviation. The O_3 response to long-lived CH_4 changes, here $d[O_3]/d[CH_4] = 3.5 \pm 1.0 \text{ DU}(O_3)$ [ppm(CH_4)]$^{-1}$, can be calculated from models (17, this work) and is qualitatively supported by numerous studies showing that the increase in mean tropospheric O_3 since the preindustrial era is partially due to the increase in CH_4 (16). Our estimated range for the CH_4 feedback factor ($f_{CH_4} = 1.4 \pm 0.1$) includes values from models with widely varying chemical mechanisms (16, 17, this work). The final terms involve mapping the changes in green-

Table 1. Factors governing the climate impact of aviation NOx emissions

Factor, unit	Value	Uncertainty*	Source[†]
$d[O_3]_{short}/dE$	0.9	± 25%	(15)
DU(O_3) [Tg(aviation N) a^{-1}]$^{-1}$	0.6	± 15%	(19)
	0.51	± 36%[‡]	(20)
	0.74		UCI
	0.60	**± 0.15**	**Adopted**
dL_{CH_4}/dE	−2.4	± 20%	(15)
%[Tg(aviation N) a^{-1}]$^{-1}$	−1.8	± 36%	(19)
	−1.55	± 38%	(20)
	−1.7		UCI
	−1.7	**± 0.35**	**Adopted**
f_{CH_4}	1.38	± 0.05	(16)
$d \ln(CH_4 \text{ lifetime})/d \ln[CH_4]$	1.30		(17)
	1.52		UCI
	1.40	**± 0.10**	**Adopted**
$d[O_3]/d[CH_4]$	3.7	± 0.8	(16)
DU(O_3) ppm(CH_4)$^{-1}$	2.4		(17)
	3.3		UCI
	3.5	**± 1.0**	**Adopted**
$dF/d[CH_4]$	370	± 7.2%	(27)
mW m^{-2} ppm(CH_4)$^{-1}$	**370**	**± 7.2%**	**Adopted**
$dF/d[O_3]$	38[§]		(28)
mW m^{-2} DU(O_3)$^{-1}$	48[§]		(29)
	42[§]	± 12	(30)
	36	± 6	(7)
	36	**± 8**	**Adopted**

DU, Dobson unit.

*Stated uncertainties are one standard deviation (68% confidence interval).

[†]UCI values are from the UCI CTM used in this work. Adopted values are used throughout this analysis.

[‡]Model standard deviation is <25% without the single outlier model.

[§]RF calculated for preindustrial to present changes in tropospheric O_3, not aviation-specific pattern.

house gas composition to RF. For CH_4 perturbations, which are globally uniform, the RF efficiency, $dF/d[CH_4] = 370$ mW m^{-2} [ppm(CH_4)]$^{-1}$ ± 7.2%, is relatively well-known and nearly constant across all models (27). For O_3 perturbations, the RF is less well-known because the perturbation patterns themselves vary significantly between models. The RF efficiency may also differ between the short-lived and long-lived O_3 responses because they have different spatial and temporal distributions, but we adopt one value here, $dF/d[O_3] = 36 ± 8$ mW m^{-2} [DU(O_3)]$^{-1}$, because the range derived from aviation-specific model tests (7) overlaps that from studies of the preindustrial to present-day changes in O_3 RF (28–30).

Table 2 shows the values and uncertainties of all RF components obtained by propagating the adopted values in Table 1 through Eqs. **1**–**4**. For simplicity, the uncertainty calculations here assume that all factors are uncorrelated, which is reasonable for the individual O_3 and CH_4 RF components, but not for their sum, as we discuss in the next section. Each one of the RF estimates derived from the factor decomposition agrees with the model ensemble estimate within its 68% confidence intervals. Furthermore, neglecting net RF for the moment, the uncertainties of each RF component derived from the factor decomposition are comparable to the standard deviations of the model ensemble. This level of agreement illustrates the usefulness of the factor decomposition method, which might be extended to RF of aviation contrails by considering factors such as flight paths, likelihood of ice supersaturation, and rates of ice sedimentation and evaporation, among others, but such an analysis is beyond the scope of this work.

An additional benefit of the factor decomposition, which is not available from the model ensemble approach, is that we can easily determine which of the terms contributes most to uncertainty in RF. For the short-lived O_3 response, uncertainties in $d[O_3]_{short}/dE$ and $dF/d[O_3]$ contribute roughly equally to the uncertainty in

Table 2. Steady-state RF (mW m^{-2}) from aviation NOx emissions, 1 Tg(N) a^{-1}

RF term	Factor decomposition*	Model ensemble[†]
Short-lived O_3	+21.6 ± 7.2	+27.3 ± 9.7
Long-lived CH_4	−15.7 ± 3.6	−16.1 ± 5.6
Long-lived O_3	−5.3 ± 2.2	−6.6 ± 3.3
Net	+0.6 ± 8.3[‡]	+4.5 ± 4.5

*Calculated from Eqs. **1**–**4** with factor values given in Table 1, assuming that all factors are uncorrelated. Stated uncertainties are one standard deviation (68% confidence interval).

[†]Calculated from models shown in Figs. 1 and 2. Stated uncertainties are one standard deviation.

[‡]Accounting for correlations due to all common factors in Eqs. **2**–**4** reduces the uncertainty to ±8.1 mW m^{-2}.

$F_{short\,O_3}$. For the long-lived CH_4 response, however, the uncertainty in dL_{CH_4}/dE causes about 80% of the uncertainty in $F_{long\,CH_4}$. In both of these cases, the dominant uncertainty originates in factors that require aviation-specific studies. In contrast, for the long-lived O_3 response, almost 50% of the variance in $F_{long\,O_3}$ originates in the $d[O_3]/d[CH_4]$ term, which reflects uncertainty in the global response of O_3 to CH_4 perturbations and is not a unique response to aviation emissions. The dL_{CH_4}/dE and $dF/d[O_3]$ uncertainties explain most of the remaining variance of long-lived O_3 RF.

Correlation of RF Components and its Causes

Fig. 2 shows the ensemble of net RF across the models. For three early studies that did not calculate $F_{long\,O_3}$, we fill in values by scaling the reported $F_{long\,CH_4}$:

Fig. 2. Steady-state net RF (mW m^{-2}) caused by aviation NOx emissions. Values are scaled to 1 Tg(N) a^{-1}. See Fig. 1 caption for the key to multimodel papers. An asterisk (*) indicates that the long-lived O_3 RF was obtained using Eq. **5**. The mean and standard deviation is given.

ENVIRONMENTAL SCIENCES

$$F_{\text{long }O_3} = F_{\text{long }CH_4}(d[O_3]/d[CH_4])(dF/d[O_3])/(dF/d[CH_4]).$$

[5]

The net RF from aviation NOx for the model ensemble is $+4.5 \pm 4.5$ mW m^{-2} for emissions of 1 Tg(N) a^{-1}. Although 17 of the 21 net RF estimates are positive, the 68% confidence interval includes zero. This range is similar to those in recent studies that use a subset of the models analyzed here [e.g., $+4.3 \pm 3.4$ (20), -0.3 to $+6.0$ (31)].

The net RF derived from the factor decomposition is $+0.6$ mW m^{-2}. If we naively assume no correlation among the RF components, then its one-sigma range is $+0.6 \pm 8.3$ mW m^{-2}, which encompasses the ensemble-based estimate and likewise spans zero. However, this assumption of no correlation gives an uncertainty in the net RF that is nearly twice as large as the spread in models, despite the similarity of standard deviations for each RF component found above. This discrepancy persists if we account for correlations due to common factors in Eqs. **2–4** (uncertainty reduces to ± 8.1 mW m^{-2}). The ensemble-derived standard deviation of net RF is also much smaller than would be expected if the variance of each of the ensemble-derived component RFs were independent (expected ± 11.6 mW m^{-2}), implying that there are important correlations between the components.

Fig. 3 shows that short-lived O_3 RF and long-lived CH_4 RF are strongly correlated in the model ensemble ($R^2 = 0.79$), which has previously been assumed but not demonstrated (15). In the absence of quantitative data, earlier work assumed 100% anticorrelation between the O_3 and CH_4 RF components, but recognized that this assumption would give confidence intervals for net aviation NOx RF that are too small (22). For example, if we assumed 100% anticorrelation, instead of the actual 79%, between the positive and negative RF components from the model ensemble, the inferred uncertainty in net RF would be ± 0.8 mW m^{-2}, which is one-fifth of the actual ensemble variation. Assuming the same with the factor decomposition, we would expect net RF uncertainty of ± 1.4 mW m^{-2}, which is one-third of the ensemble variation. Using a subset of the model ensemble studied here, Myhre et al. (7) found that the largest net aviation NOx RF occurred in models with the largest ratio of initial O_3 column change to fractional CH_4 lifetime change and the full ensemble also supports this conclusion.
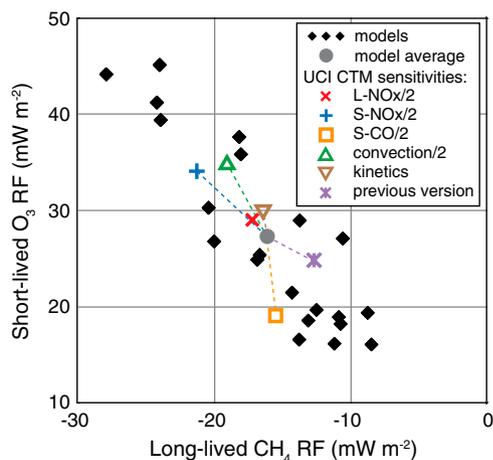
Fig. 3. Steady-state RF (mW m^{-2}) from short-lived O_3 versus long-lived CH_4 caused by aviation NOx emissions. Values are scaled to 1 Tg(N) a^{-1}. Model data (black diamonds) and their mean (gray circle) are from Fig. 1. UCI CTM sensitivity studies show change relative to the mean: lightning NOx emissions [4 Tg(N) a^{-1}] reduced 50% (L-NOx/2), surface NOx emissions (45 Tg(N) a^{-1}) reduced 50% (S-NOx/2), surface CO emissions [983 Tg(CO) a^{-1}] reduced 50% (S-CO/2), convective fluxes reduced 50% (convection/2), kinetics favoring O_3 production (kinetics), and a previous model version. Long-lived CH_4 RF here excludes the impact on stratospheric water vapor.

To assess the causes of correlation between the RF components, we test the sensitivity of the University of California, Irvine (UCI) CTM to processes and parameters that likely reflect important differences among the models in the ensemble, similar to an earlier study of global O_3 and CH_4 budgets (32). Hoor et al. (20) describe the base CTM configuration (version 5.6). RF changes in the sensitivity tests are overlaid on Fig. 3 based on factor changes given in Table S1. Large and similar changes in both short-lived O_3 and long-lived CH_4 RF components come from halving either convective fluxes or surface NOx emissions [originally 45 Tg(N) a^{-1}]. Both increase the aviation RF due to short-lived O_3 and decrease the (negative) RF due to long-lived CH_4 by 3 to 8 mW m^{-2} each. Halving the lightning NOx source [originally 4 Tg(N) a^{-1}] similarly shifts both aviation RF components in the same direction as the first perturbations but by less than 2 mW m^{-2}, possibly because most lightning occurs in the tropics far from the major flight routes. Considering the export efficiency of surface NOx to the free troposphere is 5–20% (33, 34), the changes to $d[O_3]_{\text{short}}/dE$, dL_{CH_4}/dE and RF per unit change in reactive nitrogen supply to the free troposphere agree within a factor of 3 in these sensitivity tests. In all of these tests the RF responses in the UCI CTM lie along the axis of variation for the model ensemble, indicating that varying treatments of convection, surface emissions, and lightning NOx are plausible causes of the ensemble spread and anticorrelation of aviation RFs. Prior studies show that O_3 and CH_4 RF responses to aviation NOx emissions are sensitive to the spatial variation in background NOx within a single model (8). We suggest that variation in mean tropospheric NOx between models can explain the spread of O_3 and CH_4 RFs in the ensemble.

Changes in aviation RF with temporal development of the UCI CTM (previous version 5.4) also lie along the major axis of ensemble variation, although it is unclear which changes to transport, emissions, wet deposition, and photolysis are responsible. In another sensitivity test we halve the surface CO emissions [originally 983 Tg(CO) a^{-1}]. Short-lived O_3 RF drops by 8 mW m^{-2} in response, because CO is an O_3 precursor, but the long-lived CH_4 RF changes very little, possibly because of the offsetting decrease in OH consumption by CO. To test the effect of kinetic uncertainties, we adjust rate coefficients for gas-phase reactions to the upper limit of their uncertainties (35) in favor of O_3 production from NOx ($+15\%$ for $HO_2 + NO \rightarrow OH + NO_2$, -10% for $NO + O_3 \rightarrow NO_2 + O_2$, -15% for $HO_2 + O_3 \rightarrow OH + 2O_2$). This adjustment induces small changes in both RF components. In both of these sensitivity tests the slopes of O_3 vs. CH_4 RF responses depart from the slope of the model ensemble, which suggests that variations in kinetics and CO emissions between models are not major causes of the spread in reported aviation RFs. In a final sensitivity test (not plotted), we use 2004 meteorology instead of 2005. The RF change was negligibly small for both components, indicating that interannual variability has little effect on aviation RF.

Conclusions

RF of aviation NOx emissions is often evaluated through a model ensemble approach where the standard deviation of the ensemble is used as a measure of the uncertainty. From published results, we show that one important metric, steady-state RF, has not changed much in value or uncertainty with model and emission developments over the last decade. Overall, published work suggests that the steady-state, net RF is $+4.5 \pm 4.5$ mW m^{-2} for aviation NOx emissions of 1 Tg(N) a^{-1}, which is consistent with recent studies using a subset of the models analyzed here. Other important RFs from aviation include CO_2, contrails, and induced cirrus. Current CO_2 forcing is about $+28$ mW m^{-2} for 2005 (22), but not in steady state. Contrail and cirrus RFs are typically estimated to be positive [$+33$ mW m^{-2} (22)] although some recent studies find larger positive and negative cirrus effects [-140 to

+120 mW m^{-2} (36, 37)]. These steady-state contrail and cirrus RF estimates should be increased by about 15% to compare with the 1 Tg(N) a^{-1} values used here.

The GWP allows for direct comparison of aviation emissions of NOx with those of CO$_2$. From the model ensemble here, the net RF from 1 Tg(N) aviation emission pulse integrated over 100 y is +4.5 mW a m^{-2} and that of 1 Tg of CO$_2$ is 0.087 mW a m^{-2} (derived from ref. 27). Thus, the ensemble-derived GWP of aviation NOx (as N) is 52 ± 52. If we had included the additional cooling attributed to CH$_4$-driven changes in stratospheric water vapor (7), then this number would be closer to zero, but the uncertainty would increase. Similar 100-year GWP ranges were derived by Fuglestvedt et al., (31) (−2 to 71) and Myhre et al., (7) (−21 to 67), although the latter included the stratospheric water vapor effect. Given aviation CO$_2$: NOx emission ratios of 800:1 by mass of N (7, 22), the 100-year integrated RF from aviation NOx is about 7% ± 7% of that from aviation CO$_2$.

Using a complementary approach, we factor the aviation NOx RF into its key terms and assess the best value and uncertainty of those terms, many of which reflect basic knowledge of atmospheric chemistry and RF and are not specific to aviation. The three component RF values and their uncertainties propagated from the factor decomposition, assuming no correlations among the factors, agree with the ensemble mean values and standard deviations. This second method identifies those terms largely responsible for the overall uncertainty and thus can be used to guide research priorities. For example, aviation-specific terms drive most of the uncertainty for the short-lived O$_3$ and long-lived CH$_4$ RFs—$d[O_3]_{short}/dE$, $dF/d[O_3]$, and dL_{CH_4}/dE—whereas a nonaviation term dominates for long-lived O$_3$, $d[O_3]/d[CH_4]$. The sum of the three components (i.e., net RF) derived from the factorization has twice the uncertainty of the model ensemble, when we assume that the factors are uncorrelated. Conversely, if we assume 100% anticorrelation of the positive and negative RF

components, the uncertainty in net RF is three to five times smaller than the model ensemble. The short-lived O$_3$ and long-lived CH$_4$ RF components are strongly anticorrelated ($R^2 = 0.87$) in the model ensemble, but this anticorrelation cannot be identified with the factorization. Thus, the two approaches are synergistic.

Sensitivity studies with the UCI CTM identify processes that control background NOx in the free troposphere as the likely cause of both the spread in model results and the anticorrelation between O$_3$ and CH$_4$ RFs. Simulations with less background tropospheric NOx calculated greater impacts from aviation NOx. This trend is consistent with the well-known decrease in O$_3$ production as NOx increases (e.g., 38, 39) although most aviation studies find no clear evidence of chemical nonlinearities. Improved assessments of the current and future climate impacts from aviation NOx depend on more accurate simulations of tropospheric composition, including advances in modeling convection, lightning, and surface emissions, as well as better characterization of the NOx distribution. Comparisons with NOx measurements in the free troposphere should identify which models match the observations and if these predict similar aviation impacts. However, current NOx climatologies (40) are assembled from campaigns of opportunity and do not have the necessary statistics or coverage to adequately test the models. An observational NOx climatology that includes HOx (OH + HO$_2$) sources and samples a wide range of latitudes and photochemical regimes in both hemispheres at seasonal intervals would aid process studies in global atmospheric chemistry and their application to changing emissions and climate.

1. Solomon SD, et al., ed. (2007) Summary for policymakers. *Climate Change 2007: The Physical Science Basis Fourth Assessment Report of the Intergovernmental Panel on Climate Change* (Cambridge Univ Press, Cambridge, UK), pp 1–18.
2. Gerbig C, Korner S, Lin JC (2008) Vertical mixing in atmospheric tracer transport models: Error characterization and propagation. *Atmos Chem Phys* 8:591–602.
3. Kahnert M (2008) Variational data analysis of aerosol species in a regional CTM: Background error covariance constraint and aerosol optical observation operators. *Tellus B* 60:753–770.
4. Prather MJ, Zhu X, Strahan SE, Steenrod SD, Rodriguez JM (2008) Quantifying errors in trace species transport modeling. *Proc Natl Acad Sci USA* 105:19617–19621.
5. Wang H, et al. (2009) Error correlation between CO$_2$ and CO as constraint for CO$_2$ flux inversions using satellite data. *Atmos Chem Phys* 9:7313–7323.
6. Lee DS, et al. (2010) Transport impacts on atmosphere and climate: Aviation. *Atmos Environ* 44:4678–4734.
7. Myhre G, et al. (2010) Radiative forcing due to changes in ozone and methane caused by the transport sector. *Atmos Environ* 45:387–394.
8. Stevenson DS, Derwent RG (2009) Does the location of aircraft nitrogen oxide emissions affect their climate impact? *Geophys Res Lett* 36:L17810.
9. Fuglestvedt JS, et al. (1999) Climatic forcing of nitrogen oxides through changes in tropospheric ozone and methane: Global 3D model studies. *Atmos Environ* 33:961–977.
10. Derwent RG, Collins WJ, Johnson CE, Stevenson DS (2001) Transient behavior of tropospheric ozone precursors in a global 3-D CTM and their indirect greenhouse effects. *Clim Change* 49:463–487.
11. Stevenson DS, et al. (2004) Radiative forcing from aircraft NOx emissions: Mechanisms and seasonal dependence. *J Geophys Res* 109:D17307.
12. Wild O, Prather MJ, Akimoto H (2001) Indirect long-term global radiative cooling from NOx emissions. *Geophys Res Lett* 28:1719–1722.
13. Shine KP, Berntsen TK, Fuglestvedt JS, Sausen R (2005) Scientific issues in the design of metrics for inclusion of oxides of nitrogen in global climate agreements. *Proc Natl Acad Sci USA* 102:15768–15773.
14. Berntsen TK, et al. (2005) Response of climate to regional emissions of ozone precursors: Sensitivities and warming potentials. *Tellus B* 57:283–304.
15. Penner JE, Lister DH, Griggs DJ, Dokken DJ, McFarland M (1999) *Aviation and the Global Atmosphere, Special Report of the Intergovernmental Panel on Climate Change* (Cambridge Univ Press, Cambridge, UK).
16. Prather MJ, et al. (2001) Atmospheric chemistry and greenhouse gases. *Climate Change 2001: The Scientific Basis Third Assessment Report of the Intergovernmental Panel on Climate Change*, eds JT Houghton et al. (Cambridge Univ Press, Cambridge, UK), pp 239–287.

17. Fiore AM, West JJ, Horowitz LW, Naik V, Schwarzkopf MD (2008) Characterizing the tropospheric ozone response to methane emission controls and the benefits to climate and air quality. *J Geophys Res* 113:D08307.
18. Kohler MO, et al. (2008) Impact of perturbations to nitrogen oxide emissions from global aviation. *J Geophys Res* 113:D11305.
19. Stordal F, et al. (2006) TRADEOFFs in climate effects through aircraft routing: Forcing due to radiatively active gases. *Atmos Chem Phys Discuss* 6:10733–10771.
20. Hoor P, et al. (2009) The impact of traffic emissions on atmospheric ozone and OH: Results from QUANTIFY. *Atmos Chem Phys* 9:3113–3136.
21. Sausen R, et al. (2005) Aviation radiative forcing in 2000: An update on IPCC (1999). *Meteorol Z* 14:555–561.
22. Lee DS, et al. (2009) Aviation and global climate change in the 21st century. *Atmos Environ* 43:3520–3537.
23. Unger N, et al. (2010) Attribution of climate forcing to economic sectors. *Proc Natl Acad Sci USA* 107:3382–3387.
24. Myhre G, et al. (2007) Radiative forcing due to stratospheric water vapor from CH$_4$ oxidation. *Geophys Res Lett* 34:L01807.
25. Grewe Vand Stenke A (2008) AirClim: An efficient tool for climate evaluation of aircraft technology. *Atmos Chem Phys* 8:4621–4639.
26. Wild O, Prather MJ (2000) Excitation of the primary tropospheric chemical mode in a global three-dimensional model. *J Geophys Res* 105:24647–24660.
27. Forster P, et al. (2007) Changes in atmospheric constituents and in radiative forcing. *Climate Change 2007: The Physical Science Basis Fourth Assessment Report of the Intergovernmental Panel on Climate Change*, eds S Solomon et al. (Cambridge Univ Press, Cambridge, UK), pp 129–234.
28. Haywood JM, Schwarzkopf MD, Ramaswamy V (1998) Estimates of radiative forcing due to modeled increases in tropospheric ozone. *J Geophys Res* 103:16999–17007.
29. Hauglustaine D, Brasseur G (2001) Evolution of tropospheric ozone under anthropogenic activities and associated radiative forcing of climate. *J Geophys Res* 106:32337–32360.
30. Gauss M, et al. (2003) Radiative forcing in the 21st century due to ozone changes in the troposphere and the lower stratosphere. *J Geophys Res* 108:4292.
31. Fuglestvedt JS, et al. (2010) Transport impacts on atmosphere and climate: Metrics. *Atmos Environ* 44:4648–4677.
32. Wild O (2007) Modeling the global tropospheric ozone budget: Exploring the variability in current models. *Atmos Chem Phys* 7:2643–2660.
33. Koike M, et al. (2003) Export of anthropogenic reactive nitrogen and sulfur compounds from the East Asia region in spring. *J Geophys Res* 108:8789.
34. Fang Y, et al. (2010) Sensitivity of the NOy budget over the United States to anthropogenic and lightning NOx in summer. *J Geophys Res* 115:D18312.

ENVIRONMENTAL SCIENCES

35. Sander SP, et al. (2006) *Chemical Kinetics and Photochemical Data for Use in Atmospheric Studies: Evaluation Number 15, Sect 1* (JPL Publication, Pasedena, CA), pp 9–10.

36. Penner JE, Chen Y, Wang M, Liu X (2009) Possible influence of anthropogenic aerosols on cirrus clouds and anthropogenic forcing. *Atmos Chem Phys* 9:879–896.

37. Liu XH, Penner JE, Wang MH (2009) Influence of anthropogenic sulfate and black carbon on upper tropospheric clouds in the NCAR CAM3 model coupled to the IMPACT global aerosol model. *J Geophys Res* 114:D03204.

38. Lin X, Trainer M, Liu SC (1988) On the nonlinearity of the tropospheric ozone production. *J Geophys Res* 93:15879–15888.

39. Wu SL, Duncan BN, Jacob DJ, Fiore AM, Wild O (2009) Chemical nonlinearities in relating intercontinental ozone pollution to anthropogenic emissions. *Geophys Res Lett* 36:L05806.

40. Emmons LK, et al. (2000) Data composites of airborne observations of tropospheric ozone and its precursors. *J Geophys Res* 105:20497–20538.